Casimir and van der Waals forces between two plates or a sphere (lens) above a plate made of real metals

G. L. Klimchitskaya,[1,*,†] U. Mohideen,[2,‡] and V. M. Mostepanenko[1,†,§]
[1]*Physics Department, Federal University of Paraíba, Caixa Postal 5008, CEP 58059–970, João Pessoa, Paraíba, Brazil*
[2]*Department of Physics, University of California, Riverside, California 92521*
(Received 26 January 2000; published 17 May 2000)

The Casimir and van der Waals forces acting between two metallic plates or a sphere (lens) above a plate are calculated, accounting for the finite conductivity of the metals. A simple formalism of surface modes is briefly presented which makes it possible to obtain a generalization of the Lifshitz results for the case of two semispaces covered by thin layers. Additional clarification of the regularization procedure provides the means to obtain reliable results not only for the force but also for the energy density. This, in turn, leads to the value of the force for the configuration of a sphere (lens) above a plate, both of which are covered by additional layers. The Casimir interaction between Al and Au test bodies is recalculated using tabulated optical data for the complex refractive index of these metals. The computations turn out to be in agreement with perturbation theory up to fourth order in the relative penetration depth of electromagnetic zero-point oscillations into the metal. The disagreements between the results recently presented in the literature are resolved. The Casimir force between Al bodies covered by thin Au layers is computed, and the possibility of neglecting spatial dispersion effects is discussed as a function of the layer thickness. The van der Waals force is calculated including the transition region to the Casimir force. The pure nonretarded van der Waals force law between Al and Au bodies is shown to be restricted to a very narrow distance interval from 0.5 nm to (2–4) nm. More exact values of the Hamaker constant for Al and Au are determined.

PACS number(s): 12.20.Ds, 03.70.+k, 78.20.−e

I. INTRODUCTION

Recently, considerable attention has been focused on the van der Waals and Casimir forces acting between macroscopic bodies. As for the van der Waals force, interest in it has quickened owing to its application in atomic force microscopy (see, e.g., the monographs [1,2] and references therein). Interest in the Casimir force was rekindled after new experiments [3,4] where it was measured more precisely in the case of metallic test bodies.

It is common knowledge that both forces are connected with the existence of zero-point vacuum oscillations of the electromagnetic field [5,6]. For closely spaced macroscopic bodies, the virtual photon emitted by an atom of one body reaches an atom of the second body during its lifetime. The correlated oscillations of the instantaneous induced dipole moments of those atoms give rise to the nonretarded van der Waals force. The Casimir force arises when the distance between two bodies is so large that the virtual photon emitted by an atom of one body cannot reach the second body during its lifetime. Nevertheless, the correlation of the quantized electromagnetic field in the vacuum state is not equal to zero at two points where the atoms belonging to different bodies are situated. Hence nonzero correlations of the induced atomic dipole moments arise once more, resulting in the Casimir force (which is also known as the retarded van der Waals force).

As is shown in [4,7,8], the corrections to the Casimir force due to the finite conductivity of the metal and surface roughness play an important role in the proper interpretation of the measurement data. Temperature corrections, are negligible in the measurement range of [4,7,8] (the data of [3] do not support the presence of finite conductivity, surface roughness, and temperature corrections which results in disagreement with the theoretically estimated values of these corrections [7] in the measurement range of [3]). In [4,7] the values of the finite conductivity corrections to the Casimir force were found by the use of a perturbation expansion in the relative penetration depth of electromagnetic zero-point oscillations into the metal, which starts from the general Lifshitz formula [9–11]. The parameter of this expansion is $\lambda_p/(2\pi a)$, where λ_p is the effective plasma frequency of the electrons and a is the distance between interacting bodies. Note that the coefficient near the first-order correction was obtained in [12,13] and near the second-order one in [14] for the configuration of two plane parallel plates. In [3,15] the results of [12,13] and, correspondingly, [14] were modified for the configuration of a spherical lens above a plate. To do this the proximity force theorem [16] was applied. The coefficients to the third- and fourth-order terms of that expansion were first obtained in [17] for both configurations.

In applications to atomic force microscopy and the van der Waals force, the Lifshitz formula and plasma model were used in [18,19] for different configurations of a tip above a plate. In [20,21], density-functional theory along with the plasma model was used in the calculation of the van der

*On leave from North-West Polytechnical Institute, St. Petersburg, Russia. Electronic address: galina@GK1372.spb.edu
†Present address: Institute for Theoretical Physics, Leipzig University, Augustusplatz 10/11, 04109, Leipzig, Germany.
‡Electronic address: umar.mohideen@ucr.edu
§On leave from A. Friedmann Laboratory for Theoretical Physics, St. Petersburg, Russia. Electronic address: mostep@fisica.ufpb.br

Waals force. A more complicated analytical representation for the dielectric permittivity (the Drude model with approximate account of absorption bands) was used in [22] to calculate the van der Waals force with the Lifshitz formula between objects covered with a chromium layer.

The parameters of the plasma and Drude models (plasma wavelength, electronic relaxation frequency) are not known very precisely. Because of this, in [23] the attempt was undertaken to apply Lifshitz formalism numerically to gold, copper, and aluminum (see also [24]). The tabulated data for the frequency-dependent complex refractive index of these metals were used together with the dispersion relation to calculate the values of dielectric permittivity on the imaginary frequency axis. Thereupon the Casimir force was calculated in [23] for configurations of two plates and a spherical lens above a plate in a distance range from 0.05 μm to 2.5 μm. The same computation based on the Lifshitz formalism and tabulated optical data for the dielectric permittivity was repeated in [25] in a distance range from 0.1 μm to 10 μm. The two sets of results are in disagreement (see also [26]). Note that the higher-order perturbative calculations of [17] in their application range are in agreement with [25,26] but also disagree with [23,24].

In this paper we present a brief derivation of the van der Waals and Casimir energy densities and forces between two parallel metallic plates or a plate and a sphere covered with thin layers of another metal (the configuration used in the experiments [4,8]). Two plates of sufficient thickness can be modeled by two semispaces with some gap between them. The case of multilayered plane walls was considered in [27]. In contrast to [27], where the removal of the infinities of the zero-point energy was not considered, we present explicitly the details of the regularization procedure and its physical justification. We next perform an independent computation using tabulated optical data for the frequency-dependent complex refractive index of aluminum and gold with the goal of resolving the disagreement between earlier results. Our results turn out to be in agreement with [25,26] with a precision of computational error less than 1%. Also, the influence of the thin covering metallic layers on the Casimir force is determined. The range of applicability and exceptions to using the bulk metal optical data for the dielectric permittivity of the thin metallic layers are discussed. For smaller distances the intermediate (transition) region between the Casimir and van der Waals forces is examined. It is shown that the transition region is very wide, ranging from several nanometers to hundreds of nanometers. The pure van der Waals regime for aluminum and gold is restricted to separations in the interval from 0.5 nm to (2–4) nm only. More exact values of the Hamaker constant for aluminum and gold are determined with the use of the computational data obtained.

The paper is organized as follows. In Sec. II the general formalism is briefly presented, giving the Casimir and van der Waals forces including the effect of covering layers on the surface of interacting bodies (two plates or a sphere above a plate). In Sec. III the influence of the finite conductivity of the metal on the Casimir force is reexamined. Section IV contains a calculation of the Casimir force between aluminum surfaces covered by thin gold layers. In Sec. V the van der Waals force is calculated in both configurations and the transition region to the Casimir force is examined. Section VI contains a determination of the Hamaker constant values for aluminum and gold. In Sec. VII we present conclusions and discussion, in particular, of possible applications of the results obtained in experimental investigations of the Casimir force and for obtaining stronger constraints on the constants of hypothetical long-range interactions.

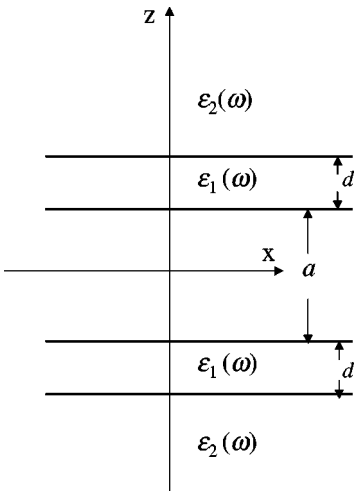

FIG. 1. The configuration of two semispaces with a dielectric permittivity $\varepsilon_2(\omega)$ covered by layers of thickness d with a permittivity $\varepsilon_1(\omega)$. The space separation between the layers is a.

II. VAN DER WAALS AND CASIMIR FORCES BETWEEN LAYERED SURFACES: GENERAL FORMALISM

We consider first two semispaces bounded by planes (x,y) and filled with material having a frequency-dependent dielectric permittivity $\varepsilon_2(\omega)$. Let the planes bounding the semispaces be covered by layers of thickness d made of another material with a dielectric permittivity $\varepsilon_1(\omega)$. The magnetic permeabilities of both materials are taken to be equal to unity. The region of thickness a between the layers (see Fig. 1) is empty space. According to [28,29] van der Waals and Casimir forces for such a configuration can be found by consideration of the surface modes for which $\mathrm{div}\,\boldsymbol{E}=0$, $\mathrm{curl}\,\boldsymbol{E}=\mathbf{0}$. The infinite zero-point energy of the electromagnetic field, dependent on a and d, is given by [5,27]

$$E(a,d)=\tfrac{1}{2}\hbar\sum_{\mathbf{k},n}\,(\omega_{\mathbf{k},n}^{(1)}+\omega_{\mathbf{k},n}^{(2)}). \tag{1}$$

Here $\omega_{\mathbf{k},n}^{(1,2)}$ are the proper frequencies of the surface modes with two different polarizations of the electric field (parallel and perpendicular to the plane formed by $\mathbf{k}$ and the z axis, respectively), and $\mathbf{k}$ is the two-dimensional propagation vector in the xy plane.

For the vacuum energy density per unit area of the bounding planes (which is also infinite) one obtains from Eq. (1)

$$\mathcal{E}(a,d)=\frac{E(a,d)}{L^2}=\frac{\hbar}{4\pi}\int_0^\infty k\,dk\sum_n\,(\omega_{\mathbf{k},n}^{(1)}+\omega_{\mathbf{k},n}^{(2)}), \quad (2)$$

where L is the side length of the bounding plane. The frequencies of the surface modes $\omega_{\mathbf{k},n}^{(1,2)}$ are found from the boundary conditions for the electric field and magnetic induction imposed at the points $z=-a/2-d$, $-a/2$, $a/2$, and $a/2+d$ [27]. These boundary conditions for each polarization lead to a system of eight linear homogeneous equations. The requirements that these equations have nontrivial solutions are

$$\Delta^{(1)}(\omega_{\mathbf{k},n}^{(1)})\equiv e^{-R_2(a+2d)}[(r_{10}^+r_{12}^+e^{R_1d}-r_{10}^-r_{12}^-e^{-R_1d})^2e^{R_0a} -(r_{10}^-r_{12}^+e^{R_1d}-r_{10}^+r_{12}^-e^{-R_1d})^2e^{-R_0a}]=0, \quad (3)$$

$$\Delta^{(2)}(\omega_{\mathbf{k},n}^{(2)})\equiv e^{-R_2(a+2d)}[(q_{10}^+q_{12}^+e^{R_1d}-q_{10}^-q_{12}^-e^{-R_1d})^2e^{R_0a} -(q_{10}^-q_{12}^+e^{R_1d}-q_{10}^+q_{12}^-e^{-R_1d})^2e^{-R_0a}]=0.$$

Here the following notations are introduced:

$$r_{\alpha\beta}^{\pm}=R_\alpha\varepsilon_\beta\pm R_\beta\varepsilon_\alpha,\quad q_{\alpha\beta}^{\pm}=R_\alpha\pm R_\beta,$$
$$R_\alpha^2=k^2-\varepsilon_\alpha\frac{\omega^2}{c^2},\quad \varepsilon_0=1,\quad \alpha=0,1,2. \quad (4)$$

Note that to obtain Eqs. (3) we set the determinants of the linear system of equations equal to zero and do not perform any additional transformations. This is the reason why Eqs. (3) do not coincide with the corresponding equations of [5,27], where some transformations were used that are not equivalent in the limit $|\omega|\to\infty$ (see below).

Summation in Eq. (2) over the solutions of Eq. (3) can be performed with the help of the argument principle which was applied for this purpose in [28]. According to this principle,

$$\sum_n\,\omega_{\mathbf{k},n}^{(1,2)}=\frac{1}{2\pi i}\left(\int_{i\infty}^{-i\infty}\omega d\ln\Delta^{(1,2)}(\omega) +\int_{C_+}\omega d\ln\Delta^{(1,2)}(\omega)\right), \quad (5)$$

where C_+ is a semicircle of infinite radius in the right half of the complex ω plane with its center at the origin. Notice that the functions $\Delta^{(1,2)}(\omega)$, defined in Eqs. (3), have no poles. For this reason the sum over their poles is absent from Eq. (5).

The second integral in the right-hand side of Eq. (5) is simply calculated with the natural supposition that

$$\lim_{\omega\to\infty}\varepsilon_\alpha(\omega)=1,\quad \lim_{\omega\to\infty}\frac{d\varepsilon_\alpha(\omega)}{d\omega}=0 \quad (6)$$

along any radial direction in the complex ω plane. The result is infinite, and does not depend on a:

$$\int_{C_+}\omega\,d\ln\Delta^{(1,2)}(\omega)=4\int_{C_+}d\omega. \quad (7)$$

Now we introduce a new variable $\xi=-i\omega$ in Eqs. (5) and (7). The result is

$$\sum_n\,\omega_{\mathbf{k},n}^{(1,2)}=\frac{1}{2\pi}\int_\infty^{-\infty}\xi\,d\ln\Delta^{(1,2)}(i\xi)+\frac{2}{\pi}\int_{C_+}d\xi, \quad (8)$$

where both contributions on the right-hand side diverge. To remove the divergences we use a regularization procedure that goes back to the original Casimir paper [30] (see also [6,28]). The idea of this procedure is that the regularized physical vacuum energy density vanishes for infinitely separated interacting bodies. From Eqs. (3) and (8) it follows that

$$\lim_{a\to\infty}\sum_n\,\omega_{\mathbf{k},n}^{(1,2)}=\frac{1}{2\pi}\int_\infty^{-\infty}\xi\,d\ln\Delta_\infty^{(1,2)}(i\xi)+\frac{2}{\pi}\int_{C_+}d\xi, \quad (9)$$

where the asymptotic behavior of $\Delta^{(1,2)}$ at $a\to\infty$ is given by

$$\Delta_\infty^{(1)}=e^{(R_0-R_2)a-2R_2d}(r_{10}^+r_{12}^+e^{R_1d}-r_{10}^-r_{12}^-e^{-R_1d})^2,$$
$$\Delta_\infty^{(2)}=e^{(R_0-R_2)a-2R_2d}(q_{10}^+q_{12}^+e^{R_1d}-q_{10}^-q_{12}^-e^{-R_1d})^2. \quad (10)$$

Now the regularized physical quantities are found with the help of Eqs. (8)–(10):

$$\left(\sum_n\,\omega_{\mathbf{k},n}^{(1,2)}\right)_{reg}\equiv\sum_n\,\omega_{\mathbf{k},n}^{(1,2)}-\lim_{a\to\infty}\sum_n\,\omega_{\mathbf{k},n}^{(1,2)} =\frac{1}{2\pi}\int_\infty^{-\infty}\xi\,d\ln\frac{\Delta^{(1,2)}(i\xi)}{\Delta_\infty^{(1,2)}(i\xi)}. \quad (11)$$

They can be transformed to a more convenient form with the help of integration by parts,

$$\left(\sum_n\,\omega_{\mathbf{k},n}^{(1,2)}\right)_{reg}=\frac{1}{2\pi}\int_{-\infty}^{\infty}d\xi\ln\frac{\Delta^{(1,2)}(i\xi)}{\Delta_\infty^{(1,2)}(i\xi)}, \quad (12)$$

where the term outside the integral vanishes.

To obtain the physical, regularized Casimir energy density one should substitute the regularized quantities (12) into Eq. (2) instead of Eq. (8) with the result

$$\mathcal{E}_{reg}(a,d)=\frac{\hbar}{4\pi^2}\int_0^\infty k\,dk\int_0^\infty d\xi[\ln Q_1(i\xi)+\ln Q_2(i\xi)], \quad (13)$$

where

$$Q_1(i\xi)\equiv\frac{\Delta^{(1)}(i\xi)}{\Delta_\infty^{(1)}(i\xi)} =1-\left(\frac{r_{10}^-r_{12}^+e^{R_1d}-r_{10}^+r_{12}^-e^{-R_1d}}{r_{10}^+r_{12}^+e^{R_1d}-r_{10}^-r_{12}^-e^{-R_1d}}\right)^2e^{-2R_0a},$$

$$Q_2(i\xi)\equiv\frac{\Delta^{(2)}(i\xi)}{\Delta_\infty^{(2)}(i\xi)}=1-\left(\frac{q_{10}^- q_{12}^+ e^{R_1 d}-q_{10}^+ q_{12}^- e^{-R_1 d}}{q_{10}^+ q_{12}^+ e^{R_1 d}-q_{10}^- q_{12}^- e^{-R_1 d}}\right)^2 e^{-2R_0 a}. \tag{14}$$

In Eq. (13) the fact that $Q_{1,2}$ are even functions of ξ has been taken into account.

For the convenience of numerical calculations below we introduce the new variable p instead of k defined by,

$$k^2=\frac{\xi^2}{c^2}(p^2-1). \tag{15}$$

In terms of p,ξ the Casimir energy density (13) takes the form

$$\mathcal{E}_{reg}(a,d)=\frac{\hbar}{4\pi^2c^2}\int_1^\infty p\,dp\int_0^\infty \xi^2\,d\xi[\ln Q_1(i\xi)+\ln Q_2(i\xi)], \tag{16}$$

where a more detailed representation for the functions $Q_{1,2}$ from Eq. (14) is

$$\begin{aligned}Q_1(i\xi)&=1-\left(\frac{(K_1-\varepsilon_1 p)(\varepsilon_2K_1+\varepsilon_1K_2)-(K_1+\varepsilon_1 p)(\varepsilon_2K_1-\varepsilon_1K_2)e^{-2\xi K_1 d/c}}{(K_1+\varepsilon_1 p)(\varepsilon_2K_1+\varepsilon_1K_2)-(K_1-\varepsilon_1 p)(\varepsilon_2K_1-\varepsilon_1K_2)e^{-2\xi K_1 d/c}}\right)^2 e^{-2\xi pa/c},\\ Q_2(i\xi)&=1-\left(\frac{(K_1-p)(K_1+K_2)-(K_1+p)(K_1-K_2)e^{-2\xi K_1 d/c}}{(K_1+p)(K_1+K_2)-(K_1-p)(K_1-K_2)e^{-2\xi K_1 d/c}}\right)^2 e^{-2\xi pa/c}.\end{aligned} \tag{17}$$

Here all permittivities depend on $i\xi$ and

$$K_\alpha=K_\alpha(i\xi)\equiv\sqrt{p^2-1+\varepsilon_\alpha(i\xi)}=\frac{c}{\xi}R_\alpha(i\xi),\qquad \alpha=1,2. \tag{18}$$

For $\alpha=0$ one has $p=cR_0/\xi$, which is equivalent to Eq. (15).

Notice that the expressions (13) and (16) give us the finite values of the Casimir energy density which is in less common use than the force. Thus in [5] no finite expression for the energy density is presented for two semispaces. In [27] the omission of infinities is performed implicitly, namely instead of Eqs. (3) the result of their division by the terms containing $\exp(R_0a)$ was presented. The coefficient near $\exp(R_0a)$, however, turns into infinity on C_+. In other words Eqs. (3) are divided by infinity. As a result the integral along C_+ is equal to zero in [27] and the quantity (2) would seem to be finite. Fortunately, this implicit division is equivalent to the regularization procedure explicitly presented above. That is why the final results obtained in [27] are indeed correct. In [11] the energy density is not considered at all.

From Eq. (16) it is easy to obtain the Casimir force per unit area acting between semispaces covered with layers:

$$F_{ss}(a,d)=-\frac{\partial\mathcal{E}_{reg}(a,d)}{\partial a}=-\frac{\hbar}{2\pi^2c^3}\int_1^\infty p^2\,dp\int_0^\infty \xi^3\,d\xi\times\left(\frac{1-Q_1(i\xi)}{Q_1(i\xi)}+\frac{1-Q_2(i\xi)}{Q_2(i\xi)}\right). \tag{19}$$

This expression coincides with Lifshitz result [9–11] for the force per unit area between semispaces with a dielectric permittivity ε_2 if the covering layers are absent. To obtain this limiting case from Eq. (19) one should put $d=0$ and $\varepsilon_1=\varepsilon_2$,

$$F_{ss}(a)=-\frac{\hbar}{2\pi^2c^3}\int_1^\infty p^2\,dp\int_0^\infty \xi^3\,d\xi\times\left\{\left[\left(\frac{K_2+\varepsilon_2 p}{K_2-\varepsilon_2 p}\right)^2 e^{2\xi pa/c}-1\right]^{-1}+\left[\left(\frac{K_2+p}{K_2-p}\right)^2 e^{2\xi pa/c}-1\right]^{-1}\right\}. \tag{20}$$

The corresponding quantity for the energy density follows from Eq. (16):

$$\mathcal{E}_{reg}(a)=\frac{\hbar}{4\pi^2c^2}\int_1^\infty p\,dp\int_0^\infty \xi^2\,d\xi\times\left\{\ln\left[1-\left(\frac{K_2-\varepsilon_2 p}{K_2+\varepsilon_2 p}\right)^2 e^{-2\xi pa/c}\right]+\ln\left[1-\left(\frac{K_2-p}{K_2+p}\right)^2 e^{-2\xi pa/c}\right]\right\}. \tag{21}$$

The other possible method to obtain the force between semispaces (but with a permittivity ε_1) is to consider the limit $d\to\infty$ in Eq. (19). In this limit we obtain once more the results (20) and (21), where K_2,ε_2 are replaced by K_1,ε_1. Note also that we do not take into account the effect of nonzero-point temperature, which is negligible for $a\ll\hbar c/T$.

The independent expression for the physical energy density is especially important because it allows one to obtain an approximate value of the force for the configuration of a sphere (or a spherical lens) above a semispace. Both bodies can be covered with layers of another material. According to the proximity force theorem, this force is

$$F_{sl}(a,d)=2\pi R\mathcal{E}_{reg}(a,d)$$
$$=\frac{\hbar R}{2\pi c^2}\int_1^\infty p\,dp\int_0^\infty \xi^2\,d\xi[\ln Q_1(i\xi)+\ln Q_2(i\xi)], \tag{22}$$

where R is the sphere radius and $Q_{1,2}$ are defined in Eq. (17). In the absence of layers $\mathcal{E}_{reg}(a,d)$ should be replaced by $\mathcal{E}_{reg}(a)$ from Eq. (21).

Although the expression (22) is not exact it allows calculation of the force with a very high accuracy. As was shown in [6] (see also [31,32]) the proximity force theorem is equivalent to additive summation of interatomic van der Waals and Casimir force potentials with a subsequent normalization of the interaction constant. As was shown in [33] the accuracy of such a method is very high (the relative error of the results obtained is less than 0.01%) if the configuration corresponds closely to two semispaces, which is the case for a sphere (lens) of a large radius $R\gg a$ above a semispace.

In the following sections the above general results will be used for computation of the Casimir and van der Waals forces acting between real metals.

III. INFLUENCE OF FINITE CONDUCTIVITY ON THE CASIMIR FORCE

Let us first consider semispaces made of aluminum or gold. Aluminum-covered interacting bodies (a plate and a lens) were used in the experiments [4,8] because of its high reflectivity for wavelengths (plate-sphere separations) larger than 100 nm. The thickness of the Al covering layer was 300 nm. This is significantly greater than the effective penetration depth of the electromagnetic zero-point oscillations into Al, which is $\delta_0=\lambda_p/(2\pi)\approx 17$ nm (see the Introduction). That is why the Al layer can be considered as infinitely thick and modeled by a semispace. In the experiment [3] the test bodies were covered by a 500 nm Au layer, which also can be considered as infinitely thick. In [4] and [8] the Al surfaces were covered, respectively, by $d<20$ nm and $d=8$ nm sputtered Au/Pd layers to reduce the oxidation processes in Al and the effect of any associated electrostatic charges. The influence of such additional thin layers on the Casimir force is discussed in Sec. IV.

The values of the force per unit area for the configuration of two semispaces and the force for a sphere above a semispace are given by Eq. (20) and Eqs. (21) and (22). For a distance a much larger than the characteristic wavelength of absorption spectra of the semispace material, λ_0, Eqs. (20) and (21) lead [11] to the following results in the case of an ideal metal ($\varepsilon_2\to\infty$)

$$F_{ss}^{(0)}(a)=-\frac{\pi^2}{240}\frac{\hbar c}{a^4},\quad F_{sl}^{(0)}(a)=-\frac{\pi^3}{360}R\frac{\hbar c}{a^3}. \tag{23}$$

To calculate numerically the corrections to Eq. (23) due to the finite conductivity of a metal we use the tabulated data for the complex index of refraction $n+ik$ as a function of frequency [34]. The values of dielectric permittivity along the imaginary axes can be expressed through $\mathrm{Im}\,\varepsilon(\omega)=2nk$ with the help of the dispersion relation [11]

$$\varepsilon(i\xi)=1+\frac{2}{\pi}\int_0^\infty\frac{\omega\,\mathrm{Im}\,\varepsilon(\omega)}{\omega^2+\xi^2}d\omega. \tag{24}$$

Here the complete tabulated refractive indices extending from 0.04 eV to 10 000 eV for Al and from 0.1 eV to 10 000 eV for Au from [34] are used to calculate $\mathrm{Im}\,\varepsilon(\omega)$. For frequencies below 0.04 eV in the case of Al and below 0.1 eV in the case of Au, the tabulated values of [34] can be extrapolated using the free electron Drude model. In this case, the dielectric permittivity along the imaginary axis is represented as

$$\varepsilon_\alpha(i\xi)=1+\frac{\omega_{p\alpha}^2}{\xi(\xi+\gamma)}, \tag{25}$$

where $\omega_{p\alpha}=(2\pi c)/\lambda_{p\alpha}$ is the plasma frequency and γ is the relaxation frequency. $\omega_p=12.5$ eV and $\gamma=0.063$ eV were used for the case of Al based on the last results in Table XI on p. 394 of [34]. In the case of Au, the analysis is not as straightforward, but proceeding in the manner outlined in [25] we obtain $\omega_p=9.0$ eV and $\gamma=0.035$ eV. While the values of ω_p and γ based on optical data from various sources might differ slightly, we have found that the resulting numerically computed Casimir forces differ by less than 1%. In fact, if for Al metal $\omega_p=11.5$ eV and $\gamma=0.05$ eV are used as in [25], the differences are extremely small. Of the values tabulated below, only the value of the force in the case of a sphere and a semispace at 0.5 μm separation is increased by 0.1%, which on round-off to the second significant figure leads to an increase of 1%. The results of numerical integration of Eq. (24) for Al (solid curve) and Au (dashed curve) are presented in Fig. 2 on a logarithmic scale. As is seen from Fig. 2, the dielectric permittivity along the imaginary axis decreases monotonically with increasing frequency [in distinction to $\mathrm{Im}\,\varepsilon(\omega)$ which possesses peaks corresponding to interband absorption].

The obtained values of the dielectric permittivity along the imaginary axis were substituted into Eqs. (20) and (22) [taking account of Eq. (21)] to calculate the Casimir force acting between real metals in configurations of two semispaces (ss) and a sphere (lens) above a semispace (sl). Numerical integration was done from an upper limit of 10^4 eV to a lower limit of 10^{-6} eV. Changes in the upper limit or lower limit by a factor of 10 led to changes of less than 0.25% in the Casimir force. If the trapezoidal rule is used in the numerical integration of Eqs. (24) the corresponding Casimir force decreases by a factor less than 0.5%. The results are presented in Fig. 3(a) (two semispaces) and in Fig. 3(b)

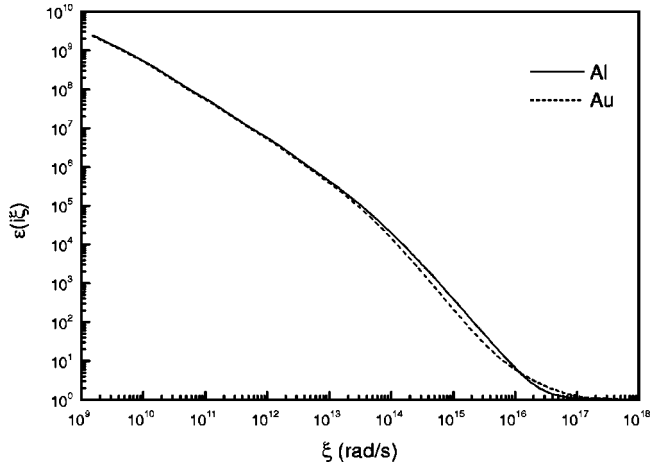

FIG. 2. The dielectric permittivity as a function of imaginary frequency for Al (solid line) and Au (dashed line).

for a sphere above a semispace by the solid lines 1 (material of the test bodies is aluminum) and 2 (material is gold). On the vertical axis the relative force $F_{ss}/F_{ss}^{(0)}$ is plotted in Fig. 3(a) and $F_{sl}/F_{sl}^{(0)}$ in Fig. 3(b). These quantities provide a sense of the correction factors to the Casimir force due to the effect of finite conductivity. In the horizontal axis the space separation is plotted in the range 0.1–1 μm. We do not present the results for larger distances because then the temperature corrections to the Casimir force become significant. At room temperature the temperature corrections contribute only 2.6% of $F_{sl}^{(0)}$ at $a=1$ μm, but at $a=3$ μm they contribute 47% of $F_{sl}^{(0)}$, and at $a=5$ μm 129% of $F_{sl}^{(0)}$ [35]. It is seen that the relative force for Al is larger than for Au at the same separation, as it should be because of the better reflectivity properties of Al.

TABLE I. The correction factor to the Casimir force due to the finite conductivity of the metal from the results of different authors and the present paper in configurations of two semispaces (ss) and a sphere (lens) above a semispace (sl).

			$F/F^{(0)}$			
Test bodies	Metal	a (μm)	[23,24]	Computation [25,26]	This paper	Perturbation theeory [17]
ss	Al	0.1	0.557	0.55	0.55	0.56
sl	Al	0.1	0.651	0.63	0.62	0.61
ss	Au	0.1		0.48	0.49	0.62
sl	Au	0.1		0.55	0.56	0.60
ss	Al	0.5		0.85	0.84	0.84
sl	Al	0.5		0.88	0.87	0.88
ss	Au	0.5	0.657	0.81	0.81	0.81
sl	Au	0.5	0.719	0.85	0.85	0.85
sl	Au	0.6	0.78	0.87	0.87	0.87
ss	Al	3		0.96	0.96	0.97
sl	Al	3		0.97	0.97	0.98
ss	Au	3		0.96	0.95	0.96
sl	Au	3		0.97	0.96	0.97

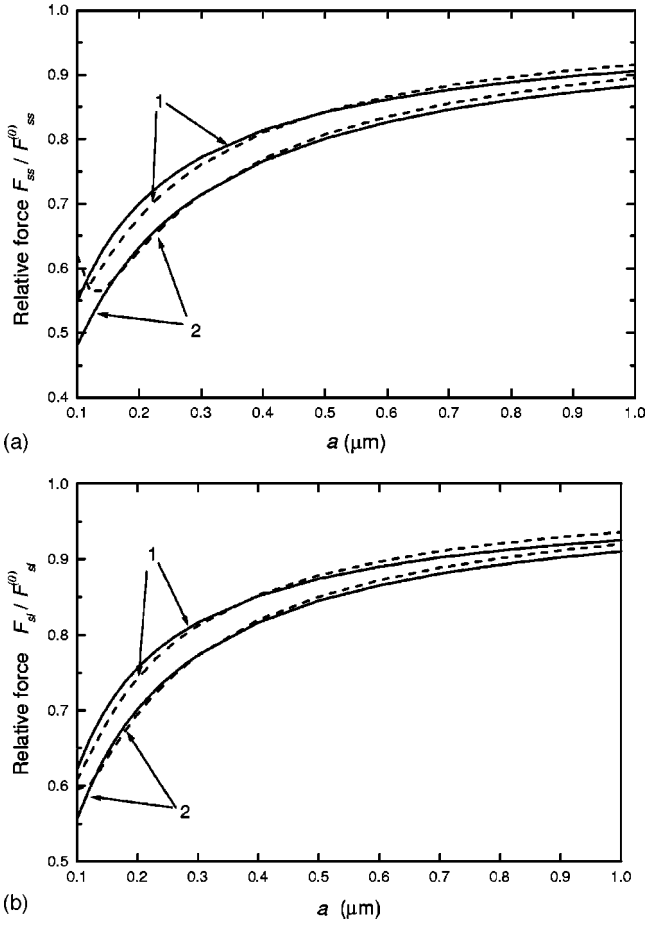

FIG. 3. The correction factor to the Casimir force due to finite conductivity of the metal as a function of the surface separation. The solid lines 1 and 2 represent the computational results for Al and Au, respectively, in the configuration of two semispaces (a) and for a sphere (lens) above a semispace (b). The dashed lines 1 and 2 represent the perturbation correction factor up to the fourth order for Al and Au, respectively.

It is interesting to compare the results obtained with those of Refs. [23,24] and [25,26] where similar computations were performed (in [25,26] analytical expressions equivalent to Eqs. (20) and (21) were used; in [23,24], however, the energy density between plates was obtained by numerical integration of the force, which can lead to some additional error). All the results for the several values of distance between the test bodies are presented in Table I.

As Table I shows, our calculational results (column 6) are in agreement with [25,26] (column 5) up to 0.01. At the same time the results of [23,24] (column 4) for Au are in disagreement with both [25,26] and this paper. The results for Al are presented in [23] at $a=0.1$ μm only. Note that the results at $a=3$ μm (the last four lines of Table I) are valid only at zero temperature. They do not take into account temperature corrections, which are significant for such separation. Also, the results of [23,24] for Cu-covered bodies are in disagreement with [25,26]. We do not consider Cu here because the outer surfaces in the recent experiments were covered with thick layers of Au [3] and Al [4,8]. The hypothesis of [24] that a Au film of 0.5 μm thickness could signifi-

cantly diffuse into a Cu layer of the same thickness at room temperatures seems unlikely. In any case it is not needed because the dielectric permittivities of Au and Cu along the imaginary axis are almost the same [17,25,26] and, consequently, will also lead to the same Casimir force.

The computational results obtained here are in good agreement with analytical perturbation expansions of the Casimir force in powers of relative penetration depth $\delta_0 = \lambda_p/(2\pi)$ of the electromagnetic zero-point oscillations into the metal. Representation (25) with $\gamma=0$ is applicable for wavelengths (space separations) larger than $\lambda_{p\alpha}$ (the corrections due to relaxation processes are small for distances $a \leqslant 5\ \mu$m). It can be substituted into Eqs. (20) and (21) to get the perturbation expansion. According to the results of Ref. [17] the relative Casimir force with finite conductivity corrections up to the fourth power is

$$\frac{F_{ss}(a)}{F_{ss}^{(0)}(a)} = 1 - \frac{16}{3}\frac{\delta_0}{a} + 24\frac{\delta_0^2}{a^2} - \frac{640}{7}\left(1 - \frac{\pi^2}{210}\right)\frac{\delta_0^3}{a^3} + \frac{2800}{9}\left(1 - \frac{163\pi^2}{7350}\right)\frac{\delta_0^4}{a^4} \tag{26}$$

for two semispaces and

$$\frac{F_{sl}(a)}{F_{sl}^{(0)}(a)} = 1 - 4\frac{\delta_0}{a} + \frac{72}{5}\frac{\delta_0^2}{a^2} - \frac{320}{7}\left(1 - \frac{\pi^2}{210}\right)\frac{\delta_0^3}{a^3} + \frac{400}{3}\left(1 - \frac{163\pi^2}{7350}\right)\frac{\delta_0^4}{a^4} \tag{27}$$

for a sphere (lens) above a semispace.

In Fig. 3(a) (two semispaces) the dashed line 1 represents the results obtained by Eq. (26) for Al with $\lambda_p = 107$ nm (which corresponds to $\omega_p = 11.5$ eV), and the dashed line 2 the results obtained by Eq. (26) for Au with $\lambda_p = 136$ nm ($\omega_p = 9$ eV) [25]. In Fig. 3(b) the dashed lines 1 and 2 represent the perturbation results obtained for Al and Au by Eq. (27) for a lens above a semispace. As we can see from the last column of Table I, the perturbation results are in good agreement (up to 0.01) with computations for all distances larger than λ_p. Only at $a = 0.1\ \mu$m for Au are there larger deviations because $\lambda_{p1} \equiv \lambda_p^{\mathrm{Au}} > 0.1\ \mu$m.

IV. CASIMIR FORCE BETWEEN LAYERED SURFACES

In this section we consider the influence of thin outer metallic layers on the Casimir force value. Let the semispaces made of Al (ε_2) be covered by Au (ε_1) layers as shown in Fig. 1. For the configuration of a sphere above a plate such a covering made of Au/Pd was used in experiments [4,8] with different values of the layer thickness d. In this case the Casimir force is given by Eqs. (19) and (22), where the quantities $Q_{1,2}(i\xi)$ are expressed by Eqs. (17) and (18). The computational results for $\varepsilon_\alpha(i\xi)$ are obtained in Sec. III from Eq. (24). Substituting them into Eqs. (19) and (22) and performing a numerical integration in the same way as above one obtains the Casimir force including the effect

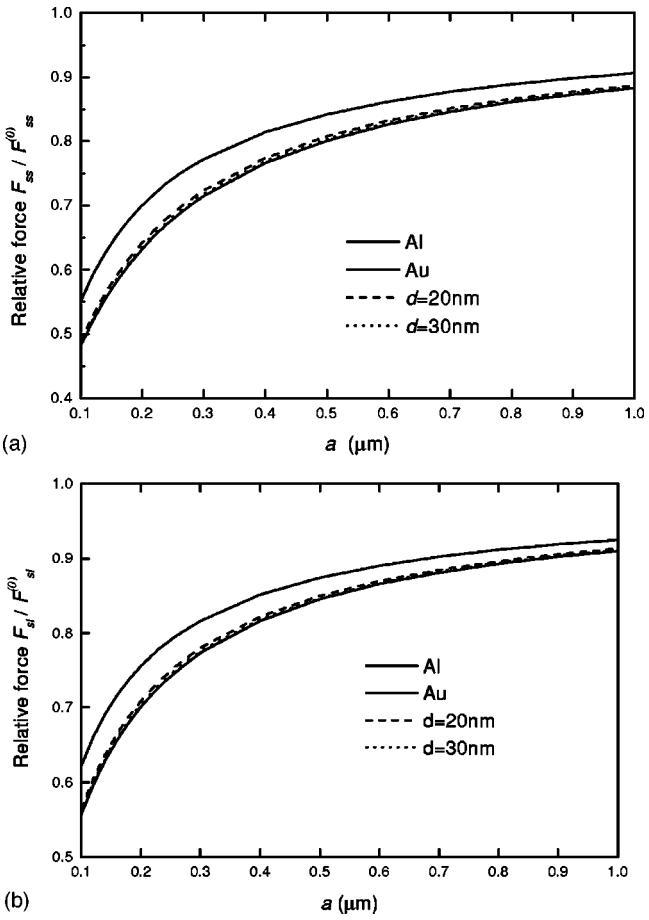

FIG. 4. The correction factor to the Casimir force due to finite conductivity of the metal as a function of the surface separation for Al test bodies covered by thin layers of Au. The dashed lines represent the results for a layer thickness $d = 20$ nm and the dotted lines for $d = 30$ nm. The case of the configuration of two semispaces is shown in (a) and for a sphere (lens) above a semispace in (b). The solid lines represent the results for pure Al and Au test bodies.

of covering layers. The computational results for a configuration of two semispaces are shown in Fig. 4(a). Here the solid lines represent once more the Casimir force between semispaces of pure Al and Au, respectively, the dashed and dotted lines are for the cases of Au layers of thickness $d = 20$ nm and $d = 30$ nm covering Al. When the layers are present, the space separation a is measured from their outer surfaces according to Eqs. (19) and (22). In Fig. 4(b) the analogous results with the same notations are presented for the configuration of a sphere (lens) above a semispace.

As Fig. 4 shows, a Au layer of $d = 20$ nm thickness significantly decreases the relative Casimir force between Al surfaces. With this layer the force approaches the value for pure Au semispaces. For a thicker Au layer of $d = 30$ nm the relative Casimir force is scarcely affected by the underlying Al. For example, at a space separation $a = 300$ nm in the configuration of two semispaces we have $F_{ss}/F_{ss}^{(0)} = 0.773$ for pure Al, $F_{ss}/F_{ss}^{(0)} = 0.727$ for Al with a 20 nm Au layer, $F_{ss}/F_{ss}^{(0)} = 0.723$ for Al with a 30 nm Au layer, and $F_{ss}/F_{ss}^{(0)} = 0.720$ for pure Au. In the same way for the configuration of a sphere above a semispace the results are

$F_{sl}/F_{sl}^{(0)}=0.817$ (pure Al), 0.780 (Al with a 20 nm Au layer), 0.776 (Al with a 30 nm Au layer), and 0.774 (pure Au). Both limiting cases $d\to\infty$ and $d\to 0$ were considered and the results are shown to coincide with those of Sec. III.

Let us now discuss the application range of the results obtained for the case of covering layers. First, from a theoretical standpoint, the main question concerns the layer thicknesses to which the formulas (19) and (22) and the above computations can be applied. In the derivation of Sec. II the spatial dispersion is neglected and, as a consequence, the dielectric permittivities ε_α depend only on ω and not on the wave vector k. In other words the field of vacuum oscillations is considered as time dependent but space homogeneous. Except for the thickness of the skin layer δ_0 the main parameters of our problem are the velocity of the electrons on the Fermi surface, v_F, the characteristic frequency of the oscillation field, ω, and the mean free path of the electrons, l. For the considered region of high frequencies (micrometer distances between the test bodies) the following conditions are valid [36]:

$$\frac{v_F}{\omega}<\delta_0\ll l. \tag{28}$$

Note that the quantity v_F/ω in the left-hand side of Eq. (28) is the distance traveled by an electron during one period of the field, so that the first inequality is equivalent to the assumption of spatial homogeneity of the oscillating field. Usually the corresponding frequencies start from the far infrared part of the spectrum, which means that the space separation $a\sim 100\,\mu$m [6]. The region of high frequencies is restricted to the short-wave optical or near ultraviolet parts of the spectrum, which correspond to surface separations of several hundred nanometers. For smaller distances absorption bands, the photoelectric effect, and other physical phenomena should be taken into account. For these phenomena, the general Eqs. (19) and (22) are still valid, however, if one substitutes the experimental tabulated data with the dielectric permittivity along the imaginary axis incorporating all these phenomena.

Now let us include one more physical parameter—the thickness d of the additional, i.e., Au, covering layer. It is evident that Eqs. (19) and (22) are applicable only for layers of such thickness that

$$\frac{v_F}{\omega}<d. \tag{29}$$

Otherwise an electron goes out of the thin layer during one period of the oscillating field and the approximation of space homogeneity is not valid. If d is so small that the inequality (29) is violated, the spatial dispersion should be taken into account, which means that the dielectric permittivity would depend not only on frequency but on a wave vector also: $\varepsilon_1=\varepsilon_1(\omega,\boldsymbol{k})$. So, if (29) is violated, the situation is analogous to the anomalous skin effect where only space dispersion is important and the inequalities below are valid:

$$\delta_0(\omega)<\frac{v_F}{\omega},\quad \delta_0(\omega)<l. \tag{30}$$

In our case, however, the role of δ_0 is played by the layer thickness d (the influence of nonlocality effects on the van der Waals force is discussed in [37,38]).

From Eqs. (28) and (29) it follows that for pure Au layers ($\lambda_p\approx 136$ nm) the space dispersion can be neglected only if $d\geqslant 25-30$ nm. For thinner layers a more general theory taking into account nonlocal effects should be developed to calculate the Casimir force. Thus for such thin layers the bulk tabulated data of the dielectric permittivity depending only on frequency cannot be used (see the experimental investigation [39], demonstrating that for Au the bulk values of dielectric constants can be obtained only from films whose thickness is about 30 nm or more). That is why the dashed lines in Fig. 4 ($d=20$ nm layers) are subject to corrections due to the influence of spatial dispersion, whereas the solid lines represent the final result. From an experimental standpoint thin layers of order a few nanometers grown by evaporation or sputtering techniques are highly porous. This is particularly so in the case of sputtered coatings as shown in [40]. The nature of the porosity is a function of the material and the underlying substrate. Thus it should be noted that the theory presented here, which used the bulk tabulated data for ε_1, cannot be applied to calculate the influence of thin covering layers of $d<20$ nm [4,7] and of $d=8$ nm [8,41] on the Casimir force. The measured high transparency of such layers for the characteristic frequencies [4,7] corresponds to a larger change of the force than what follows from Eqs. (19) and (22). This is in agreement with the qualitative analyses above.

The role of spatial dispersion was also neglected in [42], where an attempt was made to describe theoretically the influence of thin metallic covering layers on the Casimir force in experiments [4,8]. Also, the bulk materials properties were used for the Au/Pd films. As shown in [43], the resistivity of sputtered Au/Pd films even of 60 nm thickness has been shown to be extremely high, of order 2000 Ω cm. In [42] it was concluded that the maximum possible theoretical values of the force including the covering layers are significantly smaller than the measured ones. The data of [4,8], however, are shown to be consistent with a theory neglecting the influence of layers. In [4,8] the surface separations are calculated from the Al surfaces. Including the thickness of the covering layers reduces the distance between the outer surfaces, which is now smaller than the distance between the Al surfaces. Thus, contrary to [42], the theoretical value of the force should increase when the presence of the layers is included. The error made in [42] can be traced to the following. The authors of [42] changed the data of [8] ''by shifting all the points to larger separations by $2h=16$ nm'' (where $h=8$ nm is the layer thickness in [8]) instead of shifting to smaller separations by 16 nm as based on [8]. If the correct shift is done then the theoretical values of the force, including the effect of covering layers, are not smaller than the experimental values. Hence the conclusion in [42] about the probable influence of new hypothetical attractions based on the experiments [4,8] is unsubstantiated.

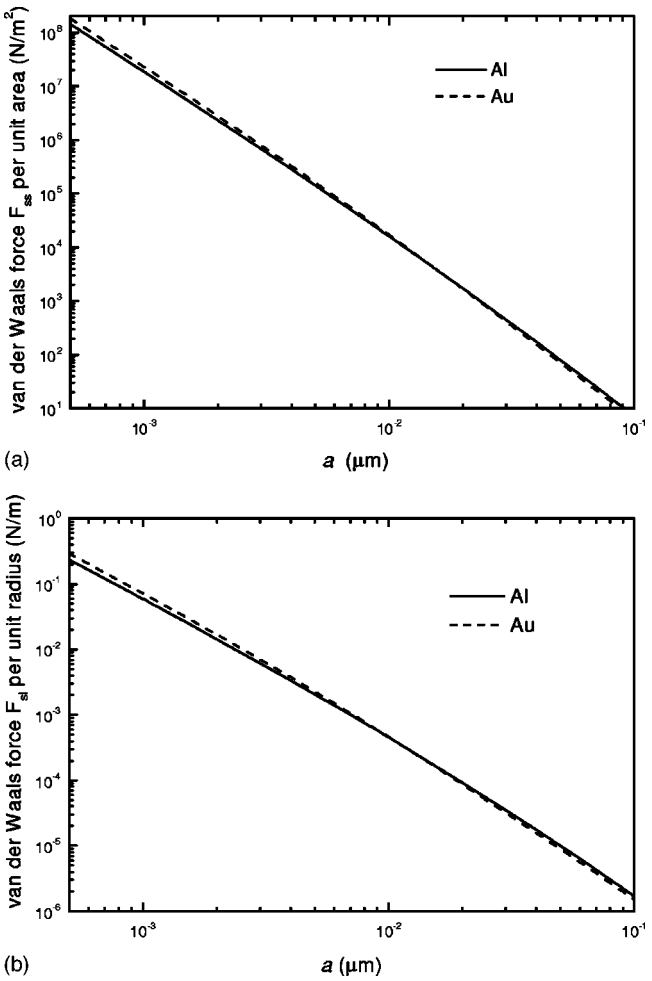

FIG. 5. The absolute value of the van der Waals force as a function of surface separation is shown on a logarithmic scale. The solid lines represent the results for Al and the dashed lines represent the case of Au. The configuration of two semispaces is shown in (a) and that for a sphere (lens) above a semispace in (b).

V. VAN DER WAALS FORCE AND INTERMEDIATE REGION

As we see from Figs. 3 and 4, at room temperature the Casimir force does not follow its ideal field-theoretical expression (23). For space separations less than $a=1\ \mu$m the corrections due to the finite conductivity of the metal are rather large [thus, at $a=1\ \mu$m they are around 7–9 % for a lens above a semispace, and 10–12 % for two semispaces; at $a=0.1\ \mu$m, around 38–44 % (sl), and 45–52 % (ss)]. For $a>1\ \mu$m the temperature corrections increase very quickly (see Sec. III). Actually, the range presented in Figs. 3 and 4 is the beginning of a transition with decreasing a from the Casimir force to the van der Waals force. Our aim is to investigate the intermediate region in more detail for smaller a and to find values of a where the pure (nonretarded) van der Waals regime starts. To do this for the case when no additional covering layers are present we numerically evaluate the integrals in Eqs. (20)–(22) for $a<100$ nm.

The computational results obtained by the same procedures as in Sec. III are presented in Figs. 5(a) for two semispaces and 5(b) for a sphere above a semispace. In both figures the solid line represents the results for aluminum test bodies, and the dashed line for gold ones. The absolute values of the van der Waals force and surface separation a are plotted along the vertical and horizontal axes on a logarithmic scale. The asymptotic expressions in the limit of $a \ll \lambda_0$ following from Eqs. (20)–(22) are [11]

$$F_{ss}^{(0)}(a)=-\frac{H}{6\pi a^3},\quad F_{sl}^{(0)}(a)=-\frac{HR}{6a^2}. \tag{31}$$

Here it is important to note that the Hamaker constant H is dependent on the material properties of the boundaries and is unknown *a priori*. This is in contrast to the ideal Casimir force limit of Eq. (23) (obtained for $a\gg\lambda_0$) which is material independent and is a function of $\hbar$ and c only. Thus it is not reasonable to express the van der Waals force as a ratio relative to Eq. (31). The asymptotic behavior described by Eq. (31) will be used below to determine the value of H.

The computations were performed with a step $\Delta a=5$ nm in the interval 10 nm$\leqslant a\leqslant$100 nm, $\Delta a=1$ nm in the interval 4 nm$\leqslant a\leqslant$10 nm, $\Delta a=0.2$ nm in the interval 2 nm $\leqslant a\leqslant$4 nm, and $\Delta a=0.1$ nm for 0.5 nm$\leqslant a\leqslant$2 nm. At $a=100$ nm the force values coincide with those in Fig. 3. For $a<0.5$ nm the repulsive exchange forces dominate. As is seen from Fig. 5 for both configurations and the two metals under consideration (Al and Au) the range of purely van der Waals force described by Eqs. (31) turns out to be extremely narrow. It extends from 0.5 nm to 2–4 nm only. For larger distances the transition from the force-distance dependence $\sim a^{-3}$ to the dependence $\sim a^{-4}$ begins (for two semispaces) and from the dependence $\sim a^{-2}$ to $\sim a^{-3}$ (for a lens above a semispace). This conclusion is in qualitative agreement with the results of [18], where the van der Waals force between a metallic sample and the metallic tip of an atomic force microscope was calculated (our choice of a sphere is formally equivalent to the paraboloidal tip considered in [18]). Calculation in [18] was performed by numerical integration of a Lifshitz-type equation for the force with the permittivity of the metal given by the plasma model [Eq. (25) with $\gamma=0$]. Strictly speaking, the plasma model is not applicable for $a \ll \lambda_0$ (see Sec. III). That is why we have used the tabulated optical data for the complex refractive index in our computations. However, the correct conclusion about the extremely narrow distance range of the purely van der Waals region for metals is obtainable by using the plasma model to represent their dielectric properties. Note that for dielectric test bodies the pure van der Waals regime extends to larger distances. For example, in the configuration of two crossed mica cylinders (which is formally equivalent to a sphere above a semispace) the van der Waals regime extends from 1.4 nm to 12 nm, as was experimentally shown in [44].

VI. DETERMINATION OF HAMAKER CONSTANTS FOR Al AND Au

The results of the previous section make it possible to determine the values of the Hamaker constant H from Eq. (31) for aluminum and gold. Let us start with the configura-

tion of two semispaces. As we see from the computational results presented in Fig. 5(a) (solid curve) the asymptotic regime for Al extends here from $a=0.5$ nm to $a=4$ nm. We use a narrower interval 0.5 nm–2 nm for the determination of n and H. The power index n of the force-distance relation given by the first formula of Eq. (31) is equal to $n=3.02\pm0.01$ in the interval considered. To obtain this value the slopes between adjacent points, i.e., 0.5–0.6 nm, 0.6–0.7 nm, etc., were calculated and then the average and the standard deviation were found. The corresponding mean value of the Hamaker constant is

$$H_{ss}^{\mathrm{Al}}=(3.67\pm0.02)\times10^{-19}\,\mathrm{J}. \tag{32}$$

Considering the computational results for Au [dashed curve of Fig. 5(a)] we find the asymptotic regime in a narrower interval 0.5 nm–2 nm with the power index $n=3.04\pm0.02$. The mean value of the Hamaker constant turns out to be equal to

$$H_{ss}^{\mathrm{Au}}=(4.49\pm0.07)\times10^{-19}\,\mathrm{J}. \tag{33}$$

For the configuration of a sphere (lens) above a semispace the results are presented in Fig. 5(b) (solid curve for Al and dashed curve for Au). In both cases the asymptotic region extends from $a=0.5$ nm to $a=2$ nm only, with the mean values of the power index in the second formula of Eq. (31) $n=2.04\pm0.02$ (Al) and $n=2.08\pm0.03$ (Au). The corresponding mean values of the Hamaker constant are

$$\begin{aligned} H_{sl}^{\mathrm{Al}}&=(3.60\pm0.06)\times10^{-19}\,\mathrm{J},\\ H_{sl}^{\mathrm{Au}}&=(4.31\pm0.14)\times10^{-19}\,\mathrm{J}. \end{aligned} \tag{34}$$

It is seen that in the case of Au and a sphere above a semispace configuration the behavior of the force shows less precise agreement with the second formula of Eq. (31).

The above results obtained for the two configurations independently give the possibility to derive new values of the Hamaker constant for Al and Au. Taking into account the value of Eq. (32) and the first expression from Eq. (34) we get

$$H^{\mathrm{Al}}=(3.6\pm0.1)\times10^{-19}\,\mathrm{J}. \tag{35}$$

The absolute error here was chosen in such a way as to cover both permitted intervals in Eqs. (32) and (34).

For Au the tolerances of the second value from Eq. (34) are two times wider than the permitted interval from Eq. (33). That is why the most probable final value of the Hamaker constant for gold can be estimated as

$$H^{\mathrm{Au}}=(4.4\pm0.2)\times10^{-19}\,\mathrm{J}. \tag{36}$$

The decreased accuracy from Eq. (35) is explained by the extremely narrow region of pure van der Waals force law for gold. These values of H for gold are compatible with those obtained previously. For example, in [45] values between 2 and 4×10^{-19} J were obtained using different procedures.

VII. CONCLUSIONS AND DISCUSSION

General expressions have been obtained for both the Casimir energy density and the force in the configuration of two plates (semispaces) with different separations between them. The case where the surfaces were covered by thin layers made of another material was also considered. Additional clarifications of the regularization procedure were given. This is important for obtaining a finite physical value for the energy density. The latter quantity is very important for obtaining the Casimir force, for the configuration of a sphere (lens) above a plate (semispace) which was used in recent experiments. For this configuration a general expression for the Casimir force taking account of layers covering a lens and a semispace, was arrived at by use of the proximity force theorem.

The Casimir force was recalculated between Al and Au test bodies for the configurations of two semispaces and a sphere (lens) above a semispace. The disagreement between the results of [23,24] and [25,26] was resolved in favor of [25,26]. Additionally, computational results were compared with the perturbation expansion up to fourth order in powers of the relative penetration depth of electromagnetic zero-point oscillations into the metal. The perturbation results are also in agreement with [25,26] and with our computations for space separations larger than a plasma wavelength of the metal under study (not much larger, as is to be expected from general considerations). We have performed computations of the Casimir force between Al test bodies covered by Au thin layers. A monotonic decrease of the correction factor to the Casimir force was observed with increase of the layer thickness. A qualitative analysis leads to the conclusion that the thickness of the layer should be large enough to allow neglect of the spatial dispersion of the dielectric permittivity and the use of tabulated bulk optical data for the complex refractive index. For the Au layers the minimal allowed thickness for such an approximation was estimated as $d=30$ nm in agreement with the experimental evidence of [39]. For smaller layer thicknesses the tabulated bulk optical data cannot be used. In this case, calculation of the Casimir force would require direct measurement of the complex refractive index for the particular metal (not only the frequency dependence but also its dependence on the wave vector).

The van der Waals force was calculated between Al and Au test bodies in configurations of two semispaces and a sphere (lens) above a semispace. The computations were performed starting from the same general expressions as in the case of the Casimir force and using the same numerical procedure and tabulated optical data. The extremely narrow region where the pure nonretarded van der Waals power-law force acts was noted. This region extends from $a=0.5$ nm to $a=2-4$ nm only. For larger distances a wide transition region starts, where the nonretarded van der Waals force described by Eq. (31) gradually transforms into the retarded van der Waals (Casimir) force from Eq. (23) when the space separation approaches the value $a=1\ \mu$m. The values of the Casimir force given by Eq. (31) are never achieved at room temperature (at $a=1\ \mu$m due to the finite conductivity of the metal, while for larger distances the temperature corrections

make a strong contribution). Using the asymptotic region of the pure nonretarded van der Waals force, values of the Hamaker constant for Al and Au were obtained. For Al the reported accuracy corresponds to a relative error of 2.8%, and for Au it is around 4.5%.

The results obtained do not exhaust all the problems connected with the role of the finite conductivity of the metal in precision measurements of the Casimir force. The main problem to be solved is investigation of corrections to the force due to thin covering layers. This would demand theoretical work on the generalization of the Lifshitz formalism for the case when the spatial dispersion can be important, in addition to the frequency dependence. Also, new measurements of the complex refractive index are needed for the layers under consideration. What is more, the finite conductivity corrections to the Casimir force should be considered, together with the corrections due to the surface roughness (see, e.g., [7], where the nonadditivity of both influential factors is demonstrated) and to finite temperature. This combined research is necessary for both applied and fundamental applications of the Casimir effect. It is known that measurements of the Casimir force provide the possibility to obtain strong constraints for the constants of long-range interactions and light elementary particles predicted by the unified gauge theories, supersymmetry, and supergravity [6]. Such information is unique and cannot be obtained even by means of the most powerful modern accelerators. In Ref. [35] the constraints for Yukawa-type hypothetical interactions were strengthened up to 30 times in some distance range on the basis of the Casimir force measurements of Ref. [3]. The increased precision of the Casimir force in [4] provided the possibility to strengthen constraints up to 140 times on Yukawa-type interactions at smaller distances [46]. It is highly probable that new measurements of the Casimir force with increased accuracy will serve as an important alternative source of information about elementary particles and fundamental interactions.

ACKNOWLEDGMENTS

G.L.K. and V.M.M. are grateful to the members of the Department of Physics of the Federal University of Paraiba, where this work was partly done, for their hospitality.

[1] D. Sarid, *Scanning Force Microscopy, with Applications to Electric, Magnetic and Atomic Forces* (Oxford University Press, New York, 1994).
[2] R. Wiesendanger, *Scanning Probe Microscopy and Spectroscopy* (Cambridge University Press, Cambridge, England, 1994).
[3] S. K. Lamoreaux Phys. Rev. Lett. **78**, 5 (1997).
[4] U. Mohideen and A. Roy, Phys. Rev. Lett. **81**, 4549 (1998).
[5] P. W. Milonni, *The Quantum Vacuum* (Academic Press, San Diego, 1994).
[6] V. M. Mostepanenko and N. N. Trunov, *The Casimir Effect and Its Applications* (Clarendon Press, Oxford, 1997).
[7] G. L. Klimchitskaya, A. Roy, U. Mohideen, and V. M. Mostepanenko, Phys. Rev. A **60**, 3487 (1999).
[8] A. Roy, C. Y. Lin, and U. Mohideen, Phys. Rev. D **60**, R111101 (1999).
[9] E. M. Lifshitz, Zh. Eksp. Teor. Fiz. **29**, 94 (1956) [Sov. Phys. JETP **2**, 73 (1956)].
[10] I. E. Dzyaloshinskii, E. M. Lifshitz, and L. P. Pitaevskii, Usp. Fiz. Nauk **73**, 381 (1961) [Sov. Phys. Usp. **4**, 153 (1961)].
[11] E. M. Lifshitz and L. P. Pitaevskii, *Statistical Physics* (Pergamon Press, Oxford, 1980), Part 2.
[12] C. M. Hargreaves, Proc. K. Ned. Akad. Wet., Ser. B: Phys. Sci. **68**, 231 (1965).
[13] J. Schwinger, L. L. DeRaad, Jr., and K. A. Milton, Ann. Phys. (N.Y.) **115**, 1 (1978).
[14] V. M. Mostepanenko and N. N. Trunov, Yad. Fiz. **42**, 1297 (1985) [Sov. J. Nucl. Phys. **42**, 818 (1985)].
[15] V. B. Bezerra, G. L. Klimchitskaya, and C. Romero, Mod. Phys. Lett. A **12**, 2613 (1997).
[16] J. Blocki, J. Randrup, W. J. Swiatecki, and C. F. Tsang, Ann. Phys. (N.Y.) **105**, 427 (1977).
[17] V. B. Bezerra, G. L. Klimchitskaya, and V. M. Mostepanenko, Phys. Rev. A (to be pubished); e-print quant-ph/9912090.
[18] U. Hartmann, Phys. Rev. B **42**, 1541 (1990).
[19] U. Hartmann, Phys. Rev. B **43**, 2404 (1991).
[20] Y. Andersson, D. C. Langreth, and B. I. Lundqvist, Phys. Rev. Lett. **76**, 102 (1996).
[21] E. Hult, Y. Andersson, and B. I. Lundqvist, Phys. Rev. Lett. **77**, 2029 (1996).
[22] P. H. G. M. van Blokland and J. T. G. Overbeek, J. Chem. Soc., Faraday Trans. 1 **74**, 2637 (1978).
[23] S. K. Lamoreaux, Phys. Rev. A **59**, R3149 (1999).
[24] S. K. Lamoreaux, Phys. Rev. Lett. **81**, 5475(E) (1998).
[25] A. Lambrecht and S. Reynaud, Eur. Phys. J. D **8**, 309 (2000).
[26] A. Lambrecht and S. Reynaud, Phys. Rev. Lett. (to be published).
[27] F. Zhou and L. Spruch, Phys. Rev. A **52**, 297 (1995).
[28] N. G. van Kampen, B. R. A. Nijboer, and K. Schram, Phys. Lett. **26A**, 307 (1968).
[29] K. Schram, Phys. Lett. **43A**, 283 (1973).
[30] H. B. G. Casimir, Proc. K. Ned. Akad. Wet. **51**, 793 (1948).
[31] G. L. Klimchitskaya and Yu. V. Pavlov, Int. J. Mod. Phys. A **11**, 3723 (1996).
[32] V. B. Bezerra, G. L. Klimchitskaya, and C. Romero, Phys. Rev. A **61**, 022115 (2000).
[33] M. Bordag, G. L. Klimchitskaya, and V. M. Mostepanenko, Int. J. Mod. Phys. A **10**, 2661 (1995).
[34] *Handbook of Optical Constants of Solids*, edited by E. D. Palik (Academic Press, New York, 1998).
[35] M. Bordag, B. Geyer, G. L. Klimchitskaya, and V. M. Mostepanenko, Phys. Rev. D **58**, 075003 (1998).
[36] L. D. Landau and E. M. Lifshitz, *Electrodymanics of Continuous Media* (Pergamon, Oxford, 1982).
[37] E. I. Kats, Zh. Eksp. Teor. Fiz. **73**, 212 (1977) [Sov. Phys. JETP **46**, 109 (1977)].

[38] G. Barton, Rep. Prog. Phys. **42**, 963 (1979).
[39] P. B. Johnson and R. W. Christy, Phys. Rev. B **6**, 4370 (1972).
[40] I. Stokroos, D. Kalicharan, J. J. L. Van der Want, and W. L. Jongebloed, J. Microsc. **189**, 79 (1997).
[41] A. Roy and U. Mohideen, Phys. Rev. Lett. **82**, 4380 (1999).
[42] V. B. Svetovoy and M. V. Lokhanin, e-print quant-ph/0001010.
[43] J. R. Kirtley, S. Washburn, and M. J. Brady, Phys. Rev. Lett. **60**, 1546 (1988).
[44] J. N. Israelachvili and D. Tabor, Proc. R. Soc. London, Ser. A **331**, 19 (1972).
[45] V. A. Parsegian and G. H. Weiss, J. Colloid Interface Sci. **81**, 285 (1981).
[46] M. Bordag, B. Geyer, G. L. Klimchitskaya, and V. M. Mostepanenko, Phys. Rev. D **60**, 055004 (1999).